Geomechanics and Engineering, Vol. 1, No. 2 (2009) 155-168
DOI: http://dx.doi.org/10.12989/gae.2009.1.2.155

Alterations of breakdown and collapse pressures due to material nonlinearities

Pawel A. Nawrocki†

The Petroleum Institute, Department of Petroleum Engineering,
P.O. Box 2533, Abu Dhabi, United Arab Emirates

(Received December 2, 2008, Accepted June 16, 2009)

Abstract. Breakdown pressures obtained from the classic, linear elastic breakdown model are compared with the corresponding pressures obtained using a nonlinear material model. Compression test results obtained on sandstone and siltstone are used for that purpose together with previously formulated nonlinear model which introduces elasticity functions to address nonlinear stress-strain behaviour of rocks exhibiting stress-dependent mechanical properties. Linear and nonlinear collapse pressures are also compared and it is shown that material nonlinearities have significant effect on both breakdown and collapse pressures and on tangential stresses which control breakdown pressure around a borehole. This means that the estimates of σ_H made using linear models give stress values which are different than the real values in the earth. Thus the importance of a more accurate analysis, such as provided by the nonlinear models, is emphasised. It is shown, however, that the linear elastic model does not necessarily over-predict borehole stresses and the opposite case can be true, depending on rock type and test interpretation.

Keywords: borehole; stress analysis; critical well pressures; material nonlinearities.

1. Hydraulic fracturing and breakdown pressure

Hydraulic fracturing is one of the most important operations routinely performed in contemporary Petroleum Engineering to enhance the production of oil and gas from underground reservoirs. Hydrofracturing consists in initiating, then propagating a fracture from a well using the pressure of a fluid as source of energy. Use of this technique in the petroleum industry began more than fifty years ago, cf. Clark (1949). The hydraulic fracturing test procedure is described by Kim and Franklin (1987), and by Haimson (1978). In tests where the fractures are clearly vertical, the current method of interpretation applies (Haimson and Fairhurst 1969, Guo *et al.* 1993b), and the results obtained are usually unambiguous and reliable. For cases where the fractures are horizontal, inclined, or mixed mode, appropriate solutions of the problem have been also provided, cf. Ljunggren and Amadei (1989) and Hefny and Lo (1992). Apart from well stimulations hydrofracturing has been also used for in-situ stress determination (Bae *et al.* 2007, Haimson and Fairhurst 1969). It is the only in-situ rock stress determination technique that has been successfully applied for measuring stresses at great depths in deep and very deep boreholes where the drillhole does not have to be

† Associate Professor, Corresponding author, E-mail: pnawrocki@pi.ac.ae

assumed to be vertical and oriented perpendicular to principal in-situ stress components. Other methods such as wellbore breakouts or earthquake focal mechanisms principally indicate stress directions.

An idealized pressure-time curve of the rupture-reopening sequence of a hydraulic fracturing test is shown in Fig. 1, in which the various parameters recorded during the test are defined. The peak pressure observed during the first cycle before the formation fractures and the well starts to take fluid is referred to as the breakdown pressure P_b. Breakdown pressure is an important parameter obtained during hydraulic fracturing. When a vertical fracture is induced, the maximum in-situ horizontal stress σ_H can be determined from the breakdown pressure if the minimum horizontal in-situ stress σ_h (obtained as the closure pressure after fracture extension and shut-in) and the properties of rocks such as the tensile strength T_o or the fracture toughness, are known. Fracture is initiated for a pressure P_b then propagated at a lower pressure value P_p (propagation pressure). Once a certain volume of fluid has been injected, pumping is stopped and the fracture, which is no longer supplied, begins to close.

Breakdown is a complex process affected by many parameters such as the injection rate, the fracture fluid, the wellbore size, the state of stress, and the properties of rocks. As a result, many models and fracture simulators have been put forward to analyze breakdown pressures. Models include the classic linear elastic model by Hubbert and Willis (1957), Haimson's poroelastic model (1968), the model eliminating the tensile strength by Bredehoeft *et al.* (1976), Schmitt and Zoback's model (1989), models based on fracture mechanics (Abou-Sayed *et al.* 1978, Rummel 1987, Detournay and Carbonel 1994), and many others. The most popular one, which is the classic model, is summarized further in this paper.

Hydraulic fracturing methods have not yet reached maturity and there is a far from universal consensus about which approaches, analyses and interpretations work best. Similarly, none of the existing breakdown models are generally accepted because they cannot explain all observed breakdown phenomena. Therefore, the estimation of σ_H is accorded a low level of confidence, and the prediction or analysis of breakdown pressure is still an open question (Rutqvist *et al*. 2000). Proposed

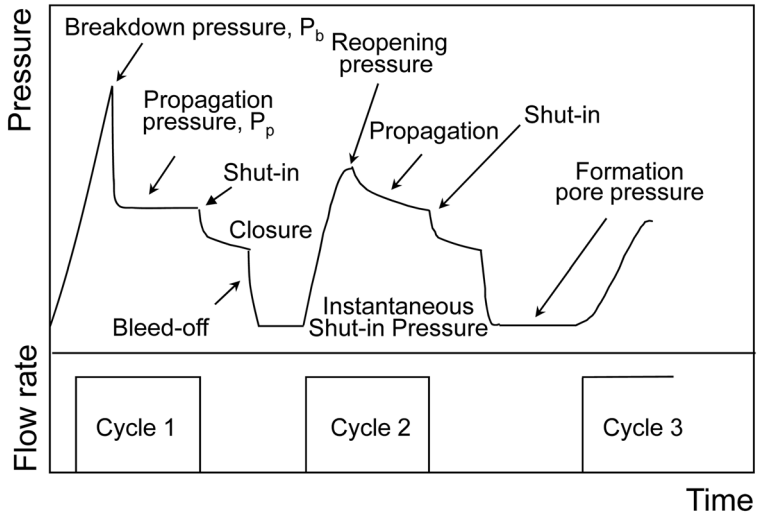

Fig. 1 Idealized hydraulic fracturing curve (after Kim and Franklin 1987)

improvements include σ_H estimations from the occurance of drilling-induced fractures (Brudy and Zoback 1999), inclusion of system stiffnes considerations (Raaen *et al.* 2001), borehole presurazition by inflation of a dilatometer (Ito *et al*. 2001), rock heterogeneity considerations (Yang *et al.* 2004), probabilistic analysis (Shin *et al.* 2001), and using the testing equipment with sufficiently low compliance (Ito *et al.* 2006). Note that at the same time, the characteristics and geometry of a hydraulic fracture at great depth are verifiable only at great expense. Due to limitations in test facilities and lack of the scale law, it is difficult to simulate the propagation of hydraulic fractures in a laboratory specimen. The reliability of a fracture model is therefore dependent on the soundness of its underlying mechanics. If the underlying mechanics in the simulator are correct, the prediction should not be far from reality.

In this paper it will be shown that nonlinear stress-strain rock properties can lead to substantial uncertainties in the estimation of σ_H from hydraulic fracturing data. The goal of this paper is to compare breakdown and collapse pressures obtained using linear and nonlinear rock models. This first step towards introducing more realistic material models into breakdown pressure analysis will be done for the isotropic in-situ stress field, $\sigma_H = \sigma_h = \sigma_{ho}$. This is partly because closed-form, nonlinear stress solutions are very hard, if not impossible, to obtain for circular openings in non-hydrostatic in-situ stress fields and it is intended to remain on the grounds of semi-analytical solutions for now. Also, this case is known to be a reasonable approximation in gravitating basins where tectonic forces are negligible, cf. Gulf Coast of USA, and it is an important limiting case. If an isotropic stress field leads to a prediction of instability, it is almost certain that an anisotropic stress field will give more dire predictions. Once the bounds of uncertainty are quantified, then anisotropic material properties and anisotropic stress fields can be later introduced through numerical methods.

2. The classic breakdown model

The classical treatment of hydraulic fracturing started with developments by Hubbert and Willis (1957). Sometimes the development of the classical equation for hydraulic fracturing is credited to them. This is not correct because they never introduced a tensile strength term in their equations. The classic model is based on Kirsch's solution (1898) for the stress distribution around a circular hole in homogeneous, isotropic, dry, linear elastic and unfractured rock subjected to external compression. In this method, the drillhole direction is assumed to be parallel to one of the principal components of the geostatic stress field. Usually, this assumption is considered valid for vertical holes drilled from the surface. Fracturing is performed in an open hole, and the fracture is a vertical plane. For the case of unequal *in-situ* horizontal stresses, $\sigma_H > \sigma_h$, two symmetric fracture wings will develop perpendicularly to the least principal stress. If the two horizontal principal stresses are equal, $\sigma_H = \sigma_h = \sigma_{ho}$, the fracture direction will be indeterminate.

The initiation pressure of a hydraulic fracture in a dry rock can easily be calculated from linear elasticity using the expression of the hoop stress at the borehole wall:

$$\sigma_\theta = (\sigma_H + \sigma_h) - 2(\sigma_H - \sigma_h)\cos 2\theta - P_w \tag{1}$$

where P_w is a well pressure. If $\theta = 0$ coincides with the direction of σ_H, then it can be seen that σ_θ varies from a maximum (compressive) value when $\theta = 90, 270$, to a minimum value achieved when $\theta = 0, 180$, and the minimum tangential stress is $\sigma_\theta|_{min} = 3\sigma_h - \sigma_H - P_w$.

Well instability can be triggered either by reducing or by increasing well pressure. Compressive rupture (shear failure) may occur at $\theta = 0$, 180 when well pressure is reduced too much. On the other hand, if well pressure is increased, the hoop stress σ_θ is reduced. It may eventually become tensile (negative) and equal to the tensile strength T_o of the rock. This initiates a hydraulic fracture in the direction of σ_H. The injection pressure at this stage is the breakdown pressure P_b, which is also called the critical pressure at fracture initiation, Fig. 1. Thus, the condition for formation of the vertical radial fracture is simply

$$\sigma_3 = T_o \tag{2}$$

or $\sigma_\theta|_{\min} = T_o$, where T_o is negative (compressive stresses are assumed to be positive in this paper). Using Eq. (1) and the fracturing criterion (2) the breakdown pressure can be calculated as:

$$P_b = 3\sigma_h - \sigma_H - T_o \tag{3}$$

Thus, breakdown pressure in a dry rock will essentially depend on the initial geostatic stresses and the tensile strength of the rock. To account for the initial pore-water pressure P_o at the test depth, Haimson (1978) applied the effective stress law and presented the following modification of Eq. (3):

$$P_b = 3\sigma_h - \sigma_H - T_o - P_o \tag{4}$$

The last equation has often been used for stress determination and is typically referred to as the conventional method. Note that pore pressure increase acts in favour of fracture initiation, as it lessens the breakdown pressure. Also note, that for the specific case $\sigma_H = \sigma_h = \sigma_{ho}$, Eq. (4) reduces to $P_b = 2\sigma_{ho} - T_o - P_o$ which predicts fracture initiation in crustal environments characterized by a lithostatic stress field or in internally pressurized thick cylinders subjected to a confining pressure σ_{ho}. Bredehoeft *et al.* (1976) eliminated tensile strength from (4) noting that T_o is an extremely variable parameter. In their modification of Eq. (4) P_b has the meaning of the fracture reopening pressure, Fig. 1, which is the peak bottomhole pressure in the second or third injection cycle. Biot's theory was used by Haimson (1968) who presented the following formula for breakdown pressure in a poroelastic material:

$$P_b = \frac{3\sigma_H - \sigma_\eta + T_o - \alpha\eta P_o}{2 - \alpha\eta} \tag{5}$$

where $\eta = (1-2\nu)/(1-\nu)$ is a function of the Poisson's ratio of the rock ν and α is Biot's poroelastic constant. The last equation was slightly modified by Schmitt and Zoback (1989) by introducing a modified effective stress law for tensile failure: $\sigma' = \sigma - \beta p$, where $0 \le \beta \le 1$.

Thus, the existing breakdown models are all based on some form of linear elastic theory although there is now general agreement that linear elasticity analyses invariably underpredict opening stability and the models which are more realistic (and less conservative) in their predictions should be utilised. These include elastoplastic and nonlinear models. Nonlinear models link rock stresses to rock deformation through experimentally determined elasticity functions rather than elastic constants, as in linear elasticity. Different nonlinear approaches postulate different mathematical representations for these functions. For example, Santarelli *et al.* (1986) introduced a confining stress dependent Young's modulus, and Nawrocki and Dusseault (1995) used the assumption of stiffness related to damage or radial distance measured from the opening wall. Note that borehole stresses predicted by linear and nonlinear methods are significantly different. Therefore, it can be expected that the constitutive material model assumed has important consequences on calculated breakdown and

collapse pressures. There are other indicators that such an approach can have merit. For example, abnormally high breakdown pressures were observed in laboratory single-well hydraulic fracture tests, Guo *et al.* (1993a). Other factors that affect wellbore collapse pressure are temperature (Wang and Dusseault 2003), chemical effects (Chen *et al.* 2003) and coupled phenomena (Fam *et al.* 2003). Phorothermoelasticity, risk analysis, time-dependent formulations, and dual porosity approach have been also used (Tao and Ghassemi 2007, Moos *et al.* 2003, Cui *et al*. 1999, Zhang *et al.* 2006 respectively). An elasto-plastic fracturing model has been formulated by Aadnoy and Belayneh (2004).

3. Method of analysis

In this article the wellbore is simulated by a hollow cylinder with R_i and R_o the inner and outer radii of the cylinder, Fig. 2. Borehole stresses σ_r and σ_θ are also defined in Fig. 2. If $R_o \to \infty$, the solution approaches that of a borehole penetrating an infinite medium. Stresses are controlled by the wellbore pressure P_w, the outer stress σ_{ho}, and the mechanical properties of the rock. Boundary stresses P_w and σ_{ho} are positive when compressive, the radial stress is σ_r, and the tangential stress is σ_θ. The radial stress component changes from the far-field stress value σ_{ho}, and on the opening wall is equal to the well pressure P_w. The critical state is reached when stresses developed at the wellbore wall satisfy either a shear failure or a fracturing criterion.

The nonlinear model used in this study for breakdown pressure calculations is the simplified version (Nawrocki *et al.* 1998) of the model introducing stress-dependent elasticity functions proposed by Nawrocki *et al.* (1996). To explicitly introduce material nonlinearities into the analysis, that model introduced a mean stress-dependent compressibility function $C(\sigma)$ and a shear stress and minimum stress-dependent inverse shear modulus function $D(\sigma_3, \tau_2)$, assuming that hydrostatic deformation is governed by $C(\sigma)$, and deviatoric deformation is governed by $D(\sigma_3, \tau_2)$. In its simplified version, the effect of minor principal stress σ_3 on material behaviour had been neglected. Such an approach is useful when limited data on material behaviour, such as only uniaxial compression test results, are available, which is often the case as the uniaxial compression test is by far the most popular test in rock mechanics. It means that the following constitutive law is used herein:

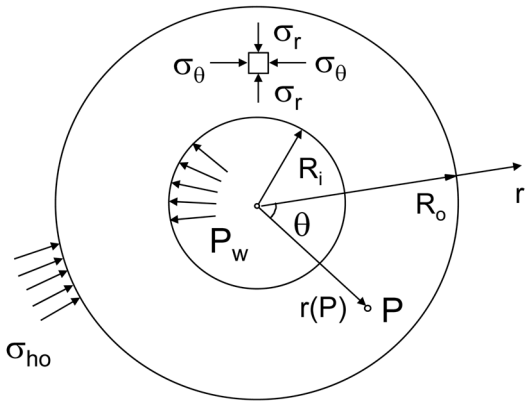

Fig. 2 Wellbore stresses and wellbore model

$$
\begin{aligned}
6\varepsilon_1 &= 2C(\sigma)\sigma - 3D(\tau_2)(\sigma - \sigma_1) \\
6\varepsilon_2 &= 2C(\sigma)\sigma - 3D(\tau_2)(\sigma - \sigma_2) \\
6\varepsilon_3 &= 2C(\sigma)\sigma - 3D(\tau_2)(\sigma - \sigma_3)
\end{aligned} \tag{6}
$$

where $\sigma_1 > \sigma_2 > \sigma_3$ are principal stresses, σ is the mean stress, $\tau_2 = ½\ (\sigma_1 - \sigma_3)$ is the shear stress, and material nonlinearities are introduced through stress-dependent functions $C(\sigma)$ and $D(\tau_2)$, which are expressed in the form of power series:

$$
\begin{aligned}
C(\sigma) &= C_o + C_1\sigma + \ldots + C_n\sigma^n = \sum_{i=0}^{n} C_i\sigma^i \\
D(\tau_2) &= D_o + D_1\tau_2 + \ldots + D_m\tau_2^m = \sum_{j=0}^{m} D_j\tau_2^j
\end{aligned} \tag{7}
$$

Note, that when series (7) are truncated at the first term, that is, when $C(\sigma) = C_o$ and $D(\tau_2) = D_o$, then the linear equations can be recovered as a special case for the constitutive law (6). Also note that parameters of the power series must be determined using compression test data.

4. Breakdown pressure calculations

Mechanical properties of sandstone and siltstone have been taken into account in collapse and breakdown pressure calculations. Cylindrical specimens 121 mm high and 61 mm in diameter made of these two rocks have been tested in uniaxial compression. Obtained results are shown in Fig. 3a (sandstone) and 3b (siltstone). The sandstone compression curve is convex upward, whereas that of the siltstone downward. Thus, at a given reference stress level σ_1^{ref}, linear approximation of a real, nonlinear, compression curve overestimates strains for siltstone ($\varepsilon_1^{LE} > \varepsilon_1^{NL}$), and underestimates strains for sandstone ($\varepsilon_1^{LE} < \varepsilon_1^{NL}$). This will have consequences on calculated nonlinear critical wellbore pressures.

Results of compression tests shown in Fig. 3 provided means for estimating constitutive parameters used both for linear and nonlinear part of this study. Note, that the power series coefficients C_i ($i = 0, 1, \ldots, n$), and D_j ($j = 0, 1, 2, \ldots, m$) in Eqs. (7) can be determined by uniaxial compression

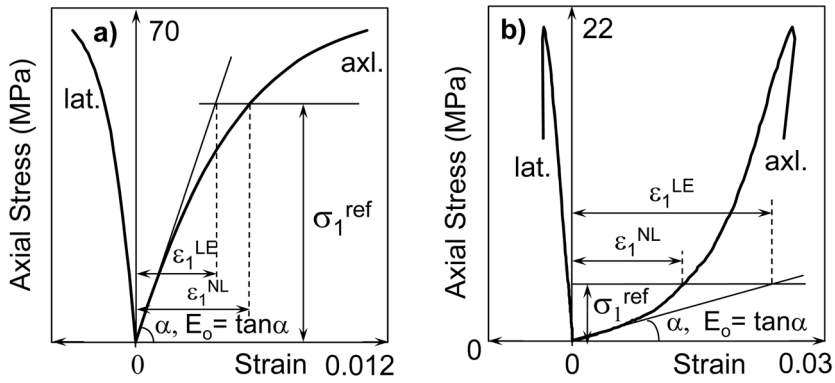

Fig. 3 Compression curves for a) sandstone, b) siltstone

tests where σ_1 is the axial compressive stress and $\sigma_2 = \sigma_3 = 0$. The strain measured in the direction of σ_1 is ε_1 and $\varepsilon_2 = \varepsilon_3$ are lateral strains. Power series coefficients C_i and D_j can be identified by plotting $\varepsilon = \varepsilon_1 + 2\varepsilon_2$ versus $\sigma = \sigma_1/3$, and $\varepsilon_1 - \varepsilon_2$ versus $\sigma_1/2$, respectively. Such format for coefficients determination results from Eqs. (6). Adding Eqs. (6) yields $\varepsilon = C(\sigma)\sigma$, whereas subtracting them results in $\varepsilon_1 - \varepsilon_2 = D(\tau_2)\tau_3$, where $\tau_3 = (\sigma_1 - \sigma_2)/2$. Note that for uniaxial compression test mean normal stress $\sigma = \sigma_1/3$, volumetric strain $\varepsilon = \varepsilon_1 + 2\varepsilon_2$, and $\tau_3 = \sigma_1/2$. Therefore Cs can be identified by plotting $\varepsilon_1 + 2\varepsilon_2$ versus $\sigma_1/3$ and Ds by plotting $\varepsilon_1 - \varepsilon_2$ versus $\sigma_1/2$. Also note that for linear materials both functions are linear. They deviate from linearity when material behaviour becomes nonlinear. Then C_o is the slope of the volumetric strain ε versus mean stress σ curve at $\sigma = 0$, and D_o is the slope of the $\varepsilon_1 - \varepsilon_2$ versus $\sigma_1/2$ curve at $\tau_2 = 0$. Therefore, the constants C_o and D_o may be viewed as the compressibility modulus and inverted shear modulus of the nonlinear material behaving linearly for very small stresses and strains. Indeed, for linear materials, the power law (7) is merely a straight line. To track nonlinear material behaviour, those lines have to become curved when the uniaxial compression curve departs from linearity. Thus, the more nonlinear material behaviour is, the more terms must be taken into account in the power series (8) to reproduce such behaviour. Using this methodology, experimental data has been presented in format allowing for Cs and Ds determination as discussed above. It has been found that four Cs and four Ds coefficients reproduce accurately compressional behaviour of sandstone, whereas five Cs and five Ds are needed for siltstone, and the specific values have been determined. As indicated above, C_o and D_o coefficients have been determined first as the initial slopes of the corresponding functions plotted as discussed. The additional coefficients have been determined by gradually increasing the number of coefficients in the power series (7) until the sufficient accuracy required to minimize the least squares error has been achieved. In this approach experimental data represent observed values and the power series (7) used in constitutive relations (6) represent values given by the model. More coefficients are required for siltstone than for sandstone because compressional behavior of silstone is more nonlinear. This can be easily verified when comparing compression curves of both rocks, Fig. 3.

The question how sensitive is the result to Cs and Ds may arise. There is major results sensitivity to increasing number of coefficient and it can be measured by qualitative and quantitative change in borehole stresses, especially the hoop stress σ_θ, obtained when the number of coefficients is increasing. For example, the quantitative change is represented by the gradual decrease of hoop stress at the borehole wall and the qualitative change by the corresponding change of the shape of the hoop stress distribution $\sigma_\theta = f(r)$ meaning that, when compared to linear material, nonlinear materials can produce the maximum hoop stress not at the borehole wall but within a rock formation, away from the borehole wall. The intensity of these effects will be different for different materials and will depend on nonlinearity level and on other parameters such as boundary conditions in terms of in situ stresses, wellbore pressures and geometry. However, for a given number of power series coefficients selected to reproduce material behavior well, the results are not that much sensitive and the sensitivity question itself becomes of secondary importance. This is because the obtained set of coefficients is by definition the best set that has to be used to model mechanical behavior of the material considered. There will be a different set, meaning a different number of coefficients and their different values, when properties of the material surrounding a wellbore change and the major qualitative and quantitative features distinct for nonlinear solution will be still there. They can be significant at times, are of the primary importance, and define the difference between linear and nonlinear analysis. Then varying the power series coefficients by a

small amount has only marginal effect on the final solution compared to the major differences already highlighted above.

With coefficients of the power series known, the nonlinear problem can be solved using the methodology discussed by Nawrocki *et al.* (1998). A basic equations set of the nonlinear problem consists of the nonlinear relations (6), the equilibrium equation, the strain compatibility equations, the strain-displacement relations, and the boundary conditions for radial stress:

$$\sigma_r = P_w @ r = R_i \text{ and } \sigma_r = \sigma_{ho} @ r = R_o \tag{8}$$

Using these equations, the nonlinear problem can be reduced to solving second-order differential equation presented in terms of radial stress σ_r and its two derivatives: $d\sigma_r/dr$, and $d^2\sigma_r/dr^2$. In the solution process, this equation is replaced by a system of first-order differential equations, which are solved using the shooting method. This method is commonly used in solving the so-called "two point boundary value problems"; that is, problems where boundary values of the unknown function are specified at two ends of the integration interval, as given by Eq. (8).

Using shooting method, the integration is begun from the left end of the integration interval, $r = R_i$, and is continued until the right end, $r = R_o$, is reached. The solution process assumes that, despite boundary conditions (8) for radial stress, the boundary value of the radial stress derivative is also known at $r = R_i$. Thus, beginning the integration at $r = R_i$, a certain value of radial stress at $r = R_o$ (shooting result) will result. That value is compared to the boundary condition at $r = R_o$. The boundary condition for radial stress derivative $d\sigma_r/dr$ at the left end of the integration interval $r = R_i$ is modified accordingly, and the process repeated until conditions (8) are satisfied. For the two rocks considered in this article the number of iterations needed did not exceed nine.

The standard hollow cylinder elastic stress solution has been used for calculating linear borehole stresses. The initial Young's modulus E_o (the modulus determined at zero strain, Fig. 3) and the corresponding initial Poisson's ratio ν_o have been used for the linear analysis together with the following equations:

$$\sigma_\theta = \frac{R_o^2(r^2 + R_i^2)\sigma_{ho} - R_i^2(r^2 + R_o^2)P_w}{r^2(R_o^2 - R_i^2)}$$
$$\sigma_r = \frac{R_o^2(r^2 - R_i^2)\sigma_{ho} - R_i^2(r^2 - R_o^2)P_w}{r^2(R_o^2 - R_i^2)} \tag{9}$$

Figs. 4 and 5 show distributions of normalized hoop stress versus normalized radius for both linear and nonlinear models. For these simulations, the borehole radius R_i and external radius R_o are assumed to be 0.3 m and 2.1 m respectively for sandstone, whereas $R_i = 0.3$ m and $R_o = 1.5$ m are assumed for siltstone. The far field stress assumed in the analysis for sandstone is $\sigma_{ho} = 10$ MPa, and several different non-penetrating well pressures, $P_w = 0$ (open hole case), $P_w = 20$, 40, and 60 MPa, have been used. The respective values for siltstone are: $\sigma_{ho} = 5$ MPa, and $P_w = 0$, $P_w = 3$, and $P_w = 6$ MPa. Both linear and nonlinear results are presented for comparison in Figs. 4 and 5.

Significant differences in σ_θ predictions are apparent: compared to a linear calculation, the nonlinear model gives lower hoop stresses for sandstone and higher for siltstone. This difference is most significant at low well pressures. Moreover, hoop stresses obtained using the nonlinear model show $\sigma_{\theta|\max}$ located not at the cylinder wall, as the linear elastic model predicts, but at some distance from the wall, Fig. 4. Hoop stress obtained using the nonlinear model is more realistic than those

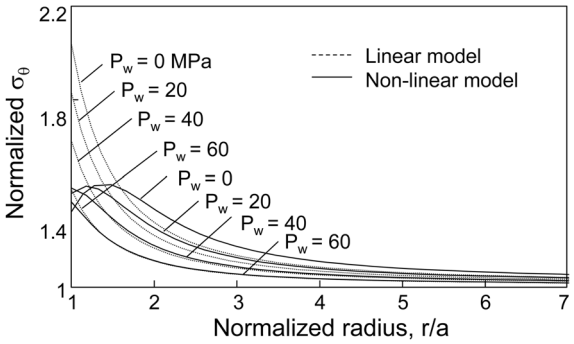

Fig. 4 Normalized hoop stress for sandstone

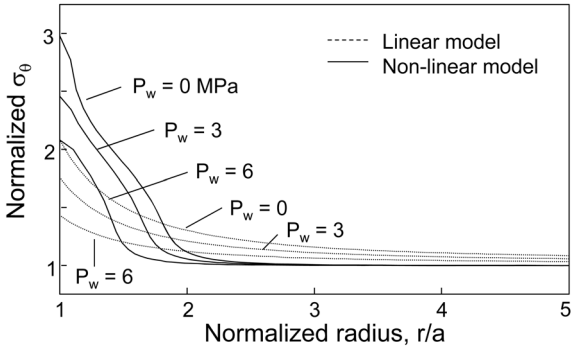

Fig. 5 Normalized hoop stress for siltstone

predicted by linear elasticity.

Obtained results have been further used for the purpose of breakdown pressure calculations. In addition, the collapse pressure P_{coll} has been also calculated. The Coulomb failure criterion has been used for calculating well collapse pressure corresponding to the onset of shear failure:

$$(\sigma_1 - \sigma_2) - (\sigma_1 + \sigma_2)\sin\varphi - 2c_o\cos\varphi = 0 \tag{10}$$

where c_o is cohesion, and φ is the angle of internal friction. Graphical representation of this criterion is shown in Fig. 6. Instead of principal stresses σ_1 and σ_2, the radial and circumferential borehole stresses are shown in Fig. 6. The tension cut-off part of the criterion has been used in breakdown pressure calculations and two stress regimes can be seen: above the hydrostatic line (shear failure criterion BD; breakdown criterion AB) hoop stress is a major principal stress $\sigma_1 = \sigma_\theta$, whereas below it (shear failure criterion FG; breakdown criterion AF) radial stress becomes a major principal stress, $\sigma_1 = \sigma_r$. Schematic stress distributions corresponding to these two regimes are also shown in Fig. 6.

The following equation specifies shear failure along BD:

$$f_1: (\sigma_\theta - \sigma_r) - (\sigma_\theta + \sigma_r)\sin\varphi - 2c_o\cos\varphi = 0 \tag{11}$$

whereas

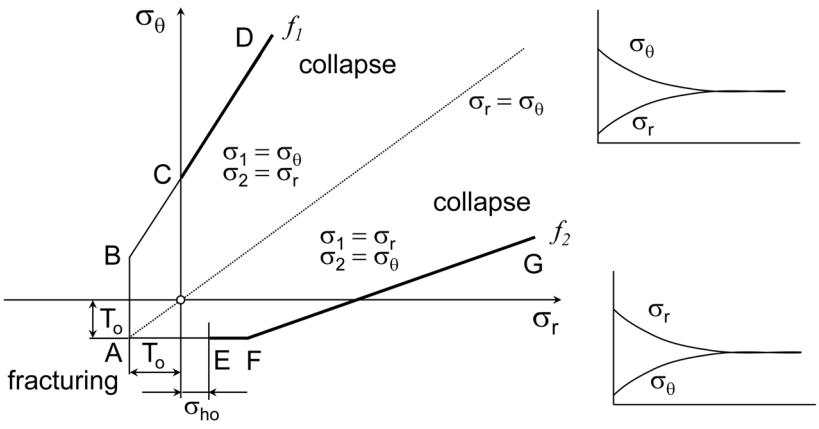

Fig. 6 Coulomb failure criterion with tension cut-off

$$f_2\colon (\sigma_\theta - \sigma_r) + (\sigma_\theta + \sigma_r)\sin\varphi + 2c_o\cos\varphi = 0 \tag{12}$$

should be used for stress combinations below the hydrostatic line. Actually, if one assumes that only positive well pressures are admissible (no suction on the wellbore wall), then only CD, FG, and EF represent the active criterion. Stress states corresponding to AB, BC, and AE are not possible because with negative well pressures excluded, the minimum well pressure is zero (open hole), *i.e.* $\sigma_{r|r=\mathrm{Ri}} = 0$. Thus, with suction excluded, f_1 shrinks to CD. Consequently, fracturing along AB is also not possible as (again, with suction excluded) radial stress at the wellbore wall cannot become tensile. On the other hand, for stress states below the hydrostatic line, AF shrinks to EF because σ_{ho} is the minimum value of well pressure for which radial stress can become a major principal stress σ_1. All stress combinations along FG are theoretically possible.

The linear elastic borehole stresses given by Eq. (9) can be readily used with breakdown criterion $\sigma_\theta = T_o$ and collapse criteria (11) and (12) to establish the limits of linear elastic solution. Thus, for linear elastic case the following equation for breakdown pressure along EF has been derived:

$$(P_b)^{\mathrm{LE}} = \frac{2R_o^2\sigma_{\mathrm{ho}} - (R_o^2 - R_i^2)T_o}{R_i^2 + R_o^2} \tag{13}$$

where T_o has to be substituted as a negative number. For wellbore penetrating an infinite medium this equation shrinks to $2\sigma_{\mathrm{ho}} - T_o$. The lower limit for breakdown pressure corresponding to the fracturing regime EF is σ_{ho} and the upper limit for the linear elastic breakdown pressure $(P_b)^{\mathrm{LE}}{}_{\max}$ is defined by radial stress corresponding to point *F*. It can be specified by calculating σ_θ from (12) and assuming $\sigma_\theta = T_o$:

$$(P_b)^{\mathrm{LE}}_{\max} = \frac{2c_o\cos\varphi + (1+\sin\varphi)T_o}{1-\sin\varphi} \tag{14}$$

For well pressure greater than the limit pressure specified above, we may have collapse corresponding to the failure criterion f_2, Eq. (12).

Accordingly, the linear elastic collapse pressure corresponding to the CD regime can be calculated by substituting $\sigma_\theta|_{r=a}$ from Eq. (9) to f_1 to obtain:

$$(P_{coll})^{\mathrm{LE}} = \frac{R_o^2(1-\sin\varphi)\sigma_{\mathrm{ho}} - c_o\cos\varphi(R_o^2 - R_i^2)}{R_o^2 - R_i^2\sin\varphi} \tag{15}$$

and the linear elastic collapse pressure corresponding to the FG regime is:

$$(P_{coll})^{\mathrm{LE}} = \frac{(R_o^2 - R_i^2)\cos\varphi + R_o^2(1+\sin\varphi)\sigma_{\mathrm{ho}}}{R_o^2 + R_i^2\sin\varphi} \tag{16}$$

The linear and nonlinear breakdown pressures are compared on Fig. 7. On this figure, the breakdown pressure has been presented as a function of σ_{ho}. It can be seen in Fig. 7, that nonlinear breakdown pressures are lower than the linear breakdown pressures for sandstone and greater than the corresponding linear pressures for siltstone. In both cases the discrepancy between the linear and nonlinear solutions increases with σ_{ho} increase.

Finally, Figs. 8 and 9 provide the comparison between linear and nonlinear collapse pressures. Fig. 8 refers to the failure regime CD, whereas linear and nonlinear collapse pressures correspond-

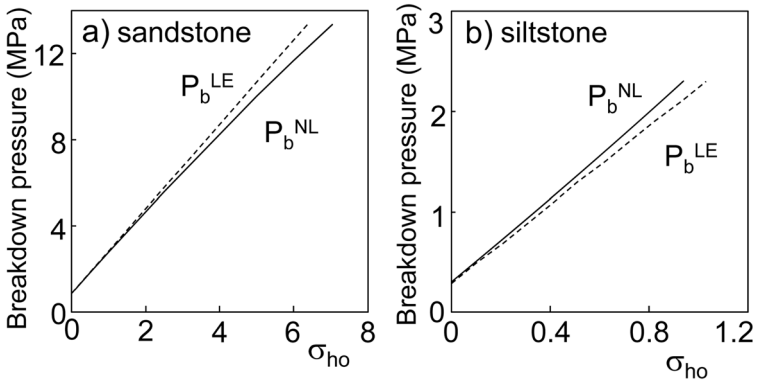

Fig. 7 Comparison of linear and nonlinear breakdown pressures

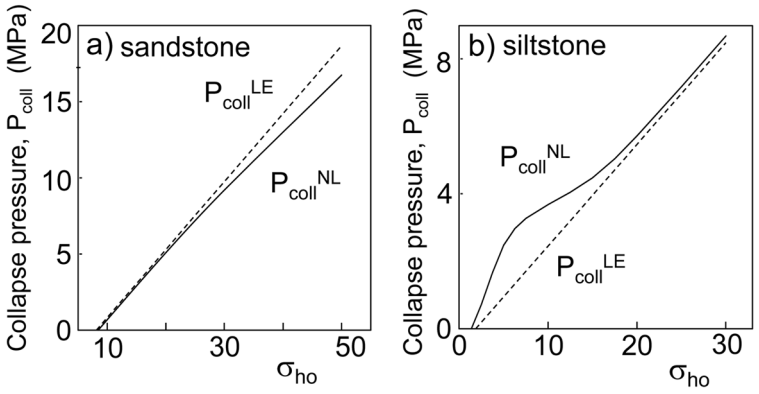

Fig. 8 Comparison of linear and nonlinear collapse pressures for stress regime CD

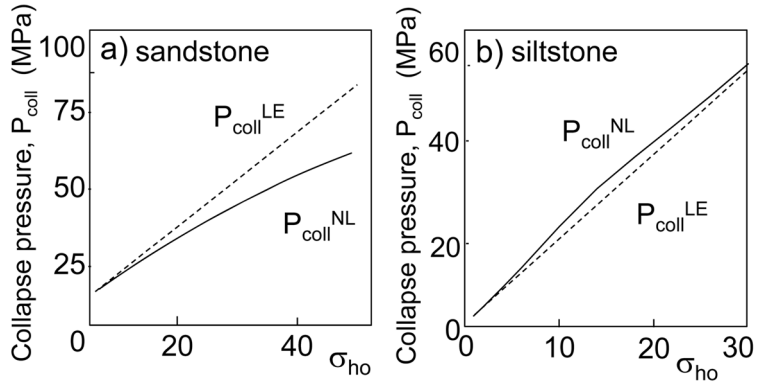

Fig. 9 Comparison of linear and nonlinear collapse pressures for stress regime FG

ing to the stress regime FG are shown in Fig. 9. It can be seen that linear elastic collapse pressure P_{coll}^{LE} is greater than nonlinear collapse pressure P_{coll}^{NL} for sandstone, and the opposite statement is true for siltstone, where the major differences between those two solutions are visible at low stresses.

5. Conclusions

Both the approach and methods of analysis presented in this paper should be effective in more robust and accurate breakdown pressure analysis than provided by the classic model. They can be used for any rock showing nonlinear behaviour in compression. A comparison between the non-linear and linear breakdown and collapse pressures done in this paper emphasises the importance of a more accurate analysis, such as provided by the nonlinear models. Obtained results show, that nonlinear model predictions are quite different from linear elastic model predictions both in terms of borehole stresses and also in terms of breakdown and collapse pressures. For the specific case of predicting tangential stresses, which control breakdown pressure around a borehole, the linear model predicts a substantially different tangential stress than the nonlinear model.

One interesting conclusion is that, contrary to common assumptions, linear elastic model does not necessarily over-predict borehole stresses. Over-predictions are common because most geomaterials tested in compression have compression curves convex upward as for the sandstone. The opposite case can be true, depending on rock type and test interpretation. Thus, results depend strongly on the constitutive model and the nonlinear model can give either higher or lower P_{b1} and P_{coll} pressures than the classic, linear elastic model. This means that the estimates of σ_H made using linear models give stress values which are different than the real values in the earth. A sensitivity analysis was carried out using varying but still reasonable degrees of nonlinearity in order to estimate the typical percentage errors that may arise in practice if conventional elastic models are used and conclude that most published data on σ_H are under-estimates of the actual values. Finding the effect of material properties significant for predicted breakdown pressures, it seems worthwhile to develop a numerical model for nonlinear breakdown pressure analysis in anisotropic in-situ stress field. Unfortunately, the development of analytical or semi-analytical solutions does not seem feasible in that case, and it looks like numerical approaches are the only option available.

References

Aadnoy, B.S. and Belayneh, M. (2004), "Elasto-plastic fracturing model for wellbore stability using non-penetrating fluids", *J. Petrol Sci. Eng.*, **45**(3-4), 179-192.

Abou-Sayed, A.S., Brechtel, C.E. and Clfton, R.J. (1978), "In-situ stress determination by hydrofracturing: a fracture mechanics approach", *J. Geophys. Res.*, **83**, 2851-2862.

Bae, S.H., Kim, J.M., Kim, J.S., Park, E.S. and Jeon, S.W. (2007), "Evaluation of initial rock stress state by hydraulic fracturing test in Korea: Overall characteristics and a case study", Rock Mechanics: *Proceedings of the 1st Canada-US Rock Mechanics Symposium* (Ed. Eberhardt, E. *et al*.), Vancouver, May, 729-736.

Bredehoeft, J.D., Wolff, R.G., Keyes, W.S. and Shuter, E. (1976), "Hydraulic fracturing to determine the regional in-situ stress field, Piceance Basin, Colorado", *Geol. Soc. Am. Bull.*, **87**, 250-258.

Brudy, M. and Zoback, M.D. (1999), "Drilling-induced tensile wall-fractures: Implications for determination of in-situ stress orientation and magnitude", *Int. J. Rock Mech. Min. Sci*., **36**(2), 191-215.

Chen, G.Z., Chenevert, M.E., Sharma, M.M. and Yu, M.J. (2003), "A study of wellbore stability in shales including poroelastic, chemical, and thermal effects", *J. Petrol Sci. Eng*., **38**(3-4), 167-176.

Clark, J.B. (1949), *Trans.* AIME, **186**, 1-3.

Cui, L., Abousleiman, Y., Cheng, A.H.D. and Roegiers, J.C. (1999), "Time-dependent failure analysis of inclined boreholes in fluid-saturated formations", *J. Energy Res. Techn.* - Trans. of the ASME, **121**(1), 31-39.

Detournay, E. and Carbonell, R. (1994), "Fracture mechanics and the breakdown process in minifrac and leak-off

tests", *Proceedings of EUROCK'94 Symposium*, Delft, August.
Fam, M.A., Dusseault, M.B. and Fooks, J.C. (2003), "Drilling in mudrocks: Rock behavior issues", *J. Petrol Sci. Eng*., **38**(3-4), 155-166.
Guo, F., Morgenstern, N.R. and Scott, J.D. (1993a), "An experimental investigation into hydraulic fracture propagation. Part I: An experimental facilities, and Part II: Single well tests", *Int. J. Rock Mech. Min. Sci. & Geomech. Abstr*., **30**(3), 177-202.
Guo, F., Morgenstern, N.R. and Scott, J.D. (1993b), "Interpretation of hydraulic fracturing breakdown pressure", *Int. J. Rock Mech. Min. Sci. & Geomech. Abstr.*, **30**(6), 617-626.
Haimson, B.C. (1968), *Hydraulic fracturing in porous and non-porous rock and its potential for determining in-situ stresses at great depth*. Ph.D. Thesis, University of Minnesota.
Haimson, B.C. and Fairhurst, C. (1969), "In-situ stress determination at great depth by means of hydraulic fracturing", *Proceedings of 11th SME of AIME Rock Mechanics Symposium*, Berkeley, June, 559-584.
Haimson, B.C. (1978), "The hydrofracturing stress measuring method and recent field results", *Int. J. Rock Mech. Min. Sci. & Geomech. Abstr.*, **15**, 167-178.
Hefny, A. and Lo, K.Y. (1992), "The interpretation of horizontal and mixed-mode fractures in hydraulic fracturing tests of rocks", *Can. Geotech. J.*, **29**(6), 902-917.
Hubbert, K.M. and Willis, D.G. (1957), "Mechanics of hydraulic fracturing", *Petrol Trans.* AIME, **210**, 153-166.
Ito, D., Sato, T.A. and Hayashi, K. (2001), "Laboratory and field verification of a new approach to stress measurements using a dilatometer tool", *Int. J. Rock Mech. Min. Sci*., **38**(8), 1173-1184.
Ito, T., Kato, H. and Tanaka, H. (2006), "Innovative concept of hydrofracturing for deep stress measurement", *Proceedings of International Symposium, In-situ Rock Stress: Measurement, Interpretation and Application,* Trondheim, June, 53-60.
Kim, K. and Franklin, J.A. (1987), "International Society for Rock Mechanics. Commission on Testing Methods. Suggested methods for rock stress determination", *Int. J. Rock Mech. Min. Sci. & Geomech. Abstr.*, **24**, 53-73.
Kirsch, G. (1898), Z. Verein Deutscher Ing. (VDI), **42**, 113.
Ljunggren, C. and Amadei, B. (1989), "Estimation of virgin rock stress from horizontal hydrofractures", *Int. J. Rock Mech. Min. Sci. & Geomech. Abstr*., **26**(1), 69-78.
Moos, D., Peska, P., Finkbeiner, T. and Zoback, M. (2003), "Comprehensive wellbore stability analysis utilizing Quantitative Risk assessment", *J. Petrol Sci. Eng.*, **38**(3-4), 97-109.
Nawrocki, P.A. and Dusseault, M.B. (1995), "Modelling of damaged zones around openings using radius-dependent Young's modulus", *Rock Mech. Rock Eng*., **28**(4), 227-239.
Nawrocki, P.A., Dusseault, M.B. and Bratli, R.K. (1996), "Semi-analytical models for predicting stresses around openings in non-linear geomaterials", *Proceedings of EUROCK'96 Turin, A.A. Balkema (Ed. Barla, G)*, Torino, September, 782-785.
Nawrocki, P.A., Dusseault, M.B. and Bratli, R.K. (1998), "Use of uniaxial compression test results in modelling stresses around openings in non-linear geomaterials", *J. Petrol Sci. Eng.*, **21**(1-2), 79-94.
Raaen, A.M., Skomedal, E., Kjorholt, H., Markestad, P. and Okland, D. (2001), "Stress determination from hydraulic fracturing tests: The system stiffness approach", *Int. J. Rock Mech. Min. Sci*., **38**(4), 529-541.
Rummel, F. (1987), *Fracture mechanics approach to hydraulic fracturing stress measurements.* Fracture Mechanics of Rock (Ed. Atkinson, B. K.), Academic Press, London.
Rutqvist, J., Tsang, C.F. and Stephansson, O. (2000), "Uncertainty in the maximum principal stress estimated from hydraulic fracturing measurements due to the presence of the induced fracture", *Int. J. Rock Mech. Min. Sci*., **37**(1-2), 107-120.
Santarelli, F., Brown, E.T. and Maury, V. (1986), "Analysis of borehole stresses using pressure-dependent linear elasticity", *Int. J. Rock Mech. Min. Sci & Geomech. Abstr*., **23**, 445-449.
Schmitt, D.R. and Zoback, M.D. (1989), "Poroelastic effects in the determination of the maximum horizontal principal stress in hydraulic fracturing tests - a proposed breakdown equation employing a modified effective stress relation for tensile failure", *Int. J. Rock Mech. Min. Sci. & Geomech. Abstr.*, **26**(6), 499-506.
Shin, K., Sugawara, K. and Okubo, S. (2001), "Application of Weibull's theory to estimating in situ maximum stress sigma(H) by hydrofracturing", *Int. J. Rock Mech. Min. Sci.*, **38**(3), 413-420.
Tao, Q. and Ghassemi, A. (2007), "Porothermoelastic analysis of wellbore failure and determination of in situ stress and rock strength", Rock Mechanics: *Proceedings of the 1st Canada-US Rock Mechanics Symposium*

(Ed. Eberhardt, E. *et al.*), Vancouver, May, 1657-1664.
Wang, Y.L. and Dusseault, M.B. (2003), "A coupled conductive-convective thermo-poroelastic solution and implications for wellbore stability", *J. Petrol Sci. Eng.*, **38**(3-4), 187-198.
Yang, T.H., Tham, L.G., Tang, C.A., Liang, Z.Z. and Tsui, Y. (2004), "Influence of heterogeneity of mechanical properties on hydraulic fracturing in permeable rocks", *Rock Mech. Rock Eng*., **37**(4), 251-275.
Zhang, J.C., Bai, M. and Roegiers, J.C. (2006), "On drilling directions for optimizing horizontal well stability using a dual-porosity poroelastic approach", *J. Petrol Sci. Eng*., **53**(1-2), 61-76.